Journal of
Experimental
Botany
www.jxb.oxfordjournals.org

RESEARCH PAPER

Nuclear magnetic resonance: a tool for imaging belowground damage caused by *Heterodera schachtii* and *Rhizoctonia solani* on sugar beet

C. Hillnhütter[1],*, R. A. Sikora[1], E. -C. Oerke[1] and D. van Dusschoten[2]

[1] Institute of Crop Science and Resource Conservation (INRES)–Phytomedicine, Rheinische Friedrich-Wilhelms-Universität Bonn, Nussallee 9, D-53115 Bonn, Germany

[2] IBG-2: Plant Sciences, Forschungszentrum Jülich, D-52425 Jülich, Germany

* To whom correspondence should be addressed. E-mail: chillnhu@uni-bonn.de

Abstract

Belowground symptoms of sugar beet caused by the beet cyst nematode (BCN) *Heterodera schachtii* include the development of compensatory secondary roots and beet deformity, which, thus far, could only be assessed by destructively removing the entire root systems from the soil. Similarly, the symptoms of *Rhizoctonia* crown and root rot (RCRR) caused by infections of the soil-borne basidiomycete *Rhizoctonia solani* require the same invasive approach for identification. Here nuclear magnetic resonance imaging (MRI) was used for the non-invasive detection of belowground symptoms caused by BCN and/or RCRR on sugar beet. Excessive lateral root development and beet deformation of plants infected by BCN was obvious 28 days after inoculation (dai) on MRI images when compared with non-infected plants. Three-dimensional images recorded at 56 dai showed BCN cysts attached to the roots in the soil. RCRR was visualized by a lower intensity of the MRI signal at sites where rotting occurred. The disease complex of both organisms together resulted in RCRR development at the site of nematode penetration. Damage analysis of sugar beet plants inoculated with both pathogens indicated a synergistic relationship, which may result from direct and indirect interactions. Nuclear MRI of plants may provide valuable, new insight into the development of pathogens infecting plants below- and aboveground because of its non-destructive nature and the sufficiently high spatial resolution of the method.

Key words: MRI, non-invasive, plant parasitic nematode, soil-borne pathogen.

Introduction

The beet cyst nematode (BCN) *Heterodera schachtii* (Schmidt) causes severe damage to sugar beets with yield losses of up to 25% and is considered the most important pest in sugar beet production worldwide (Amiri *et al.*, 2002). Second-stage juveniles (J2s) penetrate the elongation zone behind the root tip (Moriarty, 1964) and the beet (Decker, 1969). The J2s initiate the formation of giant cells (syncytium) in the roots (Bleve-Zachero and Zachero, 1987) that serve as a nurse cell and reduce intercellular and vascular transport of water and nutrients (Wyss, 1997). Belowground symptoms include development of compensa-

tory secondary roots, which result in the typical 'bearded' root symptom, as well as overall beet deformity; forking of the beet is often seen after destructive removal of the entire root system from soil (Cooke, 1987). In addition, white to brown, citrus-shaped females or cysts (Ø 2 mm) are attached to the root surface in later stages (Decker, 1969).

The soil-borne multinucleate basidiomycete *Rhizoctonia solani* Kühn [teleomorph *Thanatephorus cucumeris* (Frank) Donk] of anastomosis group (AG) 2-2IIIB is the cause of *Rhizoctonia* crown and root rot (RCRR), which may cause yield losses of up to 50% (Büttner *et al.*, 2004). Invasion of *R.*

solani into the host was reported near the petioles on the beet crown (Richards, 1921). Also, Baker (1970) and Herr (1996) concurred that *R. solani* initiated invasion of the plant at the base of the leaf petioles aboveground. Brown decay or dry rot of the beet tissue is visible on above- and belowground parts when it is infected with RCRR (Baker, 1970).

Although the nematode and fungus penetrate the beet at different sites, it would be reasonable to assume a direct interaction. The presence of *H. schachtii* is hypothesized to support *R. solani* infection due to damage caused by juvenile penetration and destruction of inter- and intracellular vascular tissue (Bergeson, 1972; Wyss, 1992). Furthermore, syncytia, energy-rich cell clusters, developed in the course of nematode attacks were reported as nutrient sources for *R. solani* (Back *et al.*, 2006). A direct interaction was proven in light microscopic investigations when *R. solani* colonized wounds of sugar beet seedlings produced by penetrations of *H. schachtii* (Polychronopoulos *et al.*, 1969). This experiment was conducted under sterile laboratory conditions in Petri dishes in the absence of soil, which is known to cause shifts in phytohormones that cause major changes to plant tissue (Eliasson and Bollmark, 1988; Hummel *et al.*, 2009). Interactions by the disease complex of *H. schachtii* and *R. solani* in plants were also demonstrated in soil under greenhouse conditions (Hillnhütter *et al.*, 2011). However, it remained unclear whether a direct or indirect interaction occurred between the two organisms when plants were grown in a more natural soil environment.

Rotting beet tissue as well as deformation of the beet and development of compensatory roots are known to change plant metabolism, which affects the sugar and water content of the storage organ (Cooke, 1987; Bloch and Hoffmann, 2005). Traditionally, destructive methods are used to extract beets and roots from soil samples to interpret plant–pathogen interactions by weighing, counting, and/or scanning the tissues to determine root weight, number of cysts, root length, or percentage of decay on beets (Nagel *et al.*, 2009). Destructive methods often lead to a loss of sensitive parts of the plants, which thereafter cannot be evaluated in more detail. Moreover, time course experiments are very complicated as destructive sampling increases variability and labour due to the higher number of individuals under investigation.

The application of nuclear magnetic resonance imaging (MRI) measurements to determine plant health status is potentially a method for non-destructive analysis of belowground plant parts (Blümler *et al.*, 2009; Jahnke *et al.*, 2009). High resolution MRI for detailed examination of plant tissues has been available for >20 years (Edzes *et al.*, 1998; Kuchenbrod *et al.*, 1995). Information that is made available by the use of MRI includes *in vivo* distribution of water flow in vascular conduits (van As and Windt, 2008). Image contrast in plants can be highlighted to show water mobility as influenced by membranes, water distribution, water diffusion, and water transport patterns (MacFall *et al.*, 1994; Scheenen, 2000; Köckenberger, 2001; Weishaupt, 2001; Gossuin *et al.*, 2010). In the present study, non-invasive MRI was tested to improve elucidation of plant–pathogen and pathogen–nematode inter-relationships.

Jahnke *et al.* (2009) already discussed the potential of using MRI to study the biotic interactions of sugar beet roots with pathogens, especially when nematodes or other soil-borne pathogens change the root structure or functioning. In fact, it should be possible not only to detect changes in root geometry, but also to visualize cysts or mature females and syncytia of *H. schachtii*. Furthermore, MRI may allow the detection of differences in water content of RCRR-infested regions compared with healthy plant parts. Hallois *et al.* (1992) observed root rot caused by *R. solani* on sugar beet using MRI, but the authors showed no results.

The objective of these experiments was to examine the potential of MRI for detection of biotic changes in sugar beet plants due to pathogen influence with special reference to the following aspects: (i) investigation of changes of root geometry due to *H. schachtii* presence; (ii) visualization of rotting symptoms caused by *R. solani*; (iii) detection of cysts and syncytia of *H. schachtii* on or in the roots; and (iv) examination of the inter-relationships between *R. solani* and *H. schachtii* in a soil environment

Materials and methods

Plant and pathogen preparation

Seeds of sugar beet (*Beta vulgaris* Döll, cultivar Alyssa, KWS GmbH, Einbeck, Germany), susceptible to *H. schachtii* and *R. solani*, were sown in polyvinyl chloride (PVC) tubes with a 54 mm inner diameter and length of 160 mm. These tubes were customized with cables and loops to place them vertically into the MRI spectrometer. Substrate in the tubes contained a 2:1 (v/v) mixture of sand (median grain size <2 mm) and Cambisol that was steam-sterilized at 121 °C for 120 min 1 d before sowing. All ferrous particles from sand and soil were removed using a strong magnet to avoid distortions of the MRI images. Plants were grown at 25/20 °C (day/night), a relative humidity of $70\pm10\%$, and a photoperiod of 12 h d^{-1} (>300 µmol $m^{-2}s^{-1}$, Phillips SGR 140, Hamburg, Germany). The experiments included four treatments: (i) non-treated/control; (ii) infection with *H. schachtii*; (iii) infection with *R. solani*; and (iv) and infection with *H. schachtii* and *R. solani*. For each treatment, five replicate plants were used and the experiment was repeated.

Heterodera schachtii and *R. solani* were added to the PVC tubes 28 d after sowing the sugar beets. Plants for treatments (ii) and (iv) were inoculated with 4000 J2s of *H. schachtii*, which were obtained from the Institutes' stock cultures. Nematodes were multiplied on *Brassica napus* Linné (cv. Akela, Feldsaaten Freudenberger, Krefeld, Germany) in greenhouse pots filled with sterilized sand. Cysts were extracted using a standard wet-screen decantation method and then transferred to Oostenbrink dishes filled with 5 mM $ZnCl_2$ solution for 7 d to stimulate J2 emergence (Oostenbrink, 1960). The J2s were collected in 25 µm size sieves (Retsch, Haan, Germany), counted under the microscope, and used directly for inoculation. Nematodes were inoculated into cavities (4 cm deep) in the soil with a pipette tip near the base of the plant.

Plants for treatments (ii) and (iv) were inoculated with *R. solani* following the protocol described by Berdugo (2009). *Rhizoctonia solani* (AG2-2 IIIB), which causes RCRR, obtained from the Plant Protection Service North Rhine-Westphalia was used. AG2-2IIIB was taken from pure isolates and, after 2 weeks growth on Petri dishes, four pieces of 7 mm in diameter were transferred under sterile conditions to Erlenmeyer flasks, containing 250 ml of PDB medium (Potato Dextrose Broth, Becton Dickinson, Franklin Lakes, NY, USA). The medium was previously autoclaved at 121 °C for 20 min. Flasks were shaken moderately at 100 rpm on

a shaker that was placed at 25 °C in the dark. After 15 d, mycelium was separated from the medium by sieving the content of the Erlenmeyer flask with a sterile 5 μm pore size filter paper. The mycelium was dripped off and subsequently homogenized in a blender (Waring products, Torrington, CT, USA) in order to make a stock solution (2 mg of *R. solani* mycelium per 1 ml of tap water). Each plant was inoculated 28 d after sowing with 3 ml of stock solution, next to the beet crown.

Evaluation of plants and pathogens

The experiments were terminated at 56 dai. The beet and lateral roots were washed free from soil and the number of nematodes per plant was determined. Afterwards, cysts were extracted by the wet-screen decantation technique with a sieve combination of 500 μm and 250 μm aperture (Ayoub, 1980). The cysts were separated from organic matter as described by Müller (1980). Cysts and organic matter residues from the 250 μm sieve were transferred to a 500 ml centrifuge tube, which was then filled with 400 ml of saturated ($\rho=1.23$ g ml^{-1}) $MgSO_4$ (Merck, Darmstadt, Germany) solution and 10–13 g of kaolin (AKW Eduard Kick GmbH, Amberg, Germany). The tubes were then centrifuged at 1860 *g* for 5 min and the supernatant containing the cysts was transferred to 15 ml homogenization tubes (Braun, Melsungen, Germany) in which they were crushed with a hand-held glass tissue homogenizer. The number of eggs and J2s per plant were counted under a stereoscope with ×40 magnification in a 2 ml RAS-Counting slide. The counting slide had sloping sides consisting of a 2 mm high plastic ring glued on a plastic plate of 75×37 mm (Hooper *et al.*, 2005).

Root, beet, and shoot fresh weights were determined for each plant. Lateral roots were removed from the beet with a scalpel and root length was measured with a root scanner (AGFA Snapscan 1236s™, Mortsel, Belgium) and the software WinRhizo Pro (Version 2004, Regent Instruments Inc., Quebec, Canada).

The severity of *R. solani* beet rot was estimated for each beet based on a scale by Zens *et al.* (2002) with: 0=healthy, no symptoms to 6=beet completely rotten, plant dead.

Nuclear magnetic resonance image acquisition

The images presented throughout this paper were acquired at the NMR facility of the IBG-2: Plant Sciences, Forschungszentrum Jülich using a 4.7 T/300 mm Varian VNMRS vertical wide-bore MRI system (Varian Inc., Oxford, UK). The main advantage of vertical systems over horizontal ones is that these magnets follow the natural orientation of most plants (and pots). In this manner, the gradients can be much closer to the plant allowing for much higher gradient strengths, which are required especially for working on plant roots in soils. The magnetic field is used to polarize the magnetic moments of protons, which can be detected by application of a (set of) r.f. pulses. Magnetic field gradients are used to modify the resonance frequency of the protons, which can be converted to positions within the sample with a Fourier transformation. Measurements are repeated hundreds of times with slight modifications to obtain a three-dimensional (3D) representation of the proton density, which is equivalent to the amount of water and exchangeable protons such as hydroxyl protons of sugar molecules. Since the signal decay (governed by T_2) depends on several microscopic variables, this can be used to detect different plant tissues. The return to the equilibrium state, governed by the T_1 relaxation time, offers another opportunity to improve contrast. The influence of these contrast mechanisms was minimized, such that the images came close to representing the water content in the beets. The only contrast optimization required was between water in the root and in the soil. By setting the so-called echo time (TE) to 9 ms, nearly all soil water signal was destroyed, whereas the signal loss of root/beet water was limited to ~30%.

During MRI measurements, which took up to 60 min, the plants were positioned in the borehole of the 4.7 T MRI system at a controlled temperature of 20 °C. One measurement was acquired using the 1.5 T MRI system that featured a split-coil magnet in order to better visualize the cysts on the beets and roots. Two types of measurements were used, both resulting in a 3D data set, namely a single echo multislice sequence (SEMS) that acquires several slices independently and a single echo 3D sequence that subdivides a selected region in a 3D voxel grid, which requires a 3D Fourier transformation as opposed to the multiple, independent 2D Fourier transformations used for the SEMS measurement (Haacke *et al.*, 1999). Images were collected at 28 and 56 dai.

The software VnmrJ™ (Varian Inc., Oxford, UK) was used to acquire images. IDL (ITT, Boulder, CO, USA) was used to analyse and display the images, 3D representations were made using MeVislab (MeVis Medical Solutions AG, Bremen, Germany).

Statistical analysis

The statistical program PASW 18 was used for analysis of data in all experiments (SPSS Inc., Chicago, IL, USA). Plant fresh weights and root length were tested for homogeneity of variance, and one-way analysis of variance (ANOVA) was used to determine if differences existed among treatments. Subgroups were separated using the Tukey's test at a probability level of $P < 0.05$.

Plant weights were further analysed by multifactorial multivariate analysis of variance (MANOVA) at a probability level of 0.01 with the factors *R. solani*, *H. schachtii*, and *R. solani*×*H. schachtii*. MANOVA was used to test for statistical significance of the interaction between the organisms (Sikora and Carter, 1987) and to determine the type of interaction.

The *R. solani* beet rot rating values and the number of eggs and J2s per plant were compared using the *t*-test ($P < 0.05$). The control and BCN treatments were excluded from the *t*-test for the *R. solani* beet rot rating, because no infection was present. Also control and *R. solani* treatments were not included in the *t*-test on J2s and eggs, because no nematodes were present in these treatments.

Synergistic damage is defined as the magnitude of host response to concurrent pathogen damage exceeding the sum of separate responses to each pathogen (Shurtleff and Averre, 1997). According to this definition, the Abbott (1925) formula was modified and calculated for plant fresh weights as the 'synergy factor' $= \frac{\Delta1(c-s)}{\{\Delta2(c-h)+\Delta3(c-r)\}}$, where $\Delta1$=the difference between the control and the disease complex treatment; *c*=plant weight of the control treatment; *s*=plant weight of the disease complex treatment; $\Delta2$=difference in weight between the control and the BCN treatment; h=plant weight of the BCN treatment; $\Delta3$=difference in weight between control and the RCRR treatment; and *r*=plant weight of the RCRR treatment (Hillnhütter *et al.*, 2011). If the synergy factor was 1 then damage was additive, and when it was >1 it was synergistic.

Results

Plant–pathogen evaluation by magnetic resonance

Non-inoculated healthy control plants resulted in the thickest beets 28 dai in the upper beet region, as demonstrated in Fig. 1A. Only a few lateral roots had been produced and the total water content was considerably higher in the control treatment (Fig. 1A). This figure is a projection image (the 3D data set was reduced to a 2D image), so the signal intensity is a measure of the thickness of the roots and the beet. In order to visualize the thinner roots, a multicoloured display scale was used. Red signifies little signal (thin roots), and blue and yellow indicate
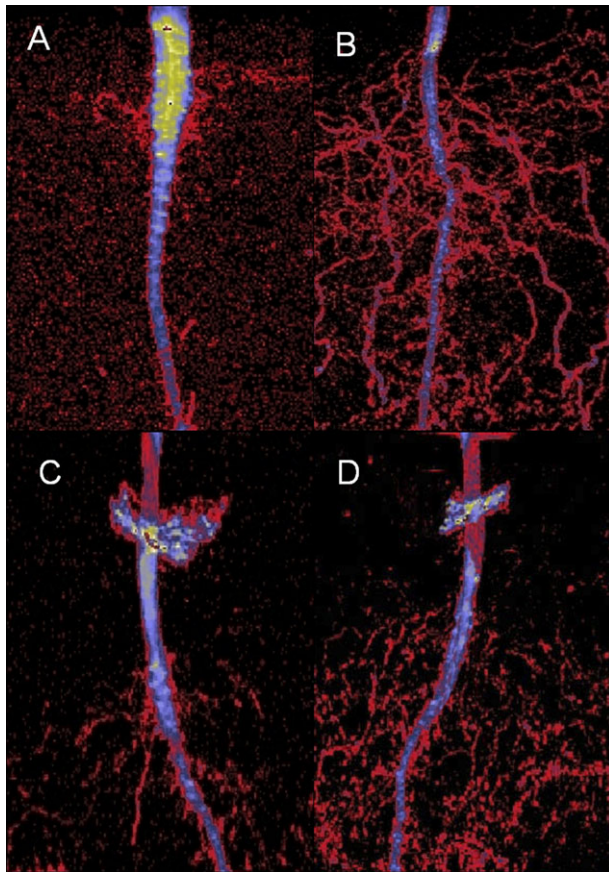
Fig. 1. Nuclear magnetic resonance image of healthy sugar beet plant (A) and plants inoculated with *Heterodera schachtii* (B); *Rhizoctonia solani* (C), and *Rhizoctonia solani* with *Heterodera schachtii* (D) 28 d after inoculation. Black, no signal; red, low signal intensity; blue, medium signal intensity; yellow-green, high signal intensity. Field of view, 80×80 mm; resolution, 210×210 µm. TE=9 ms, TR=2 s. All measured at 4.7 T.

thicker roots or regions with more water. Both effects can be separated by studying the individual slices that were used to make the projection image.

Inoculation of sugar beet with *H. schachtii* resulted in evident deviations in root and beet development from healthy plants as visualized by MRI (Fig. 1B). A considerably higher number of lateral roots was produced following nematode infection than in the control treatment. Also, the beet of the infected plant was less developed, and this resulted in a much thinner storage beet—a sign of reduced growth (Fig. 1B).

At 28 dai a circular area of high signal intensity was visible in the area where the *R. solani* inoculum had been introduced onto the soil (Fig. 1C). Root rot was detected on the beet tissue above the area of inoculation and was expressed by a decrease in signal intensity (Fig. 1C) compared with the rest of the beet. This is a clear indication of dehydration of the infected region since the overall thickness of this root section is not severely attenuated. Using the separate images, the water loss was found to be up to 85% for the region most affected by *R. solani*.

Root rot and additional lateral roots were detected on the plant inoculated with *H. schachtii* and *R. solani* concomitantly (Fig. 1D). Rotting development due to RCRR was more severe in the disease complex when compared with plants infested by RCRR alone, whereas lateral root development was less than in the BCN control (Fig. 1B, C, D).

3D images were also recorded after 56 dai and showed an advancing development of the beet organ compared with the plants recorded after 28 dai. The non-inoculated control plant showed few lateral roots and a well-developed beet (Fig. 2).

Heterodera schachtii inoculation resulted in typical deformation of the beet body and the development of thick lateral roots—the 'bearded' root symptom (Fig. 3). The dead primary root was visible in the MRI image as well as in the reference images (Fig. 3A, B). Brighter regions on the roots and small bulbs on the beet, as indicated by the arrows in the image (Fig. 3A), corresponded to the cysts attached to the roots in the reference image (Fig. 3B). There were also concentrated areas that seemed to indicate the presence of syncytia in the roots (Fig. 3). This measurement was performed using the 1.5 T magnet, since the cysts can be more easily identified at this field strength. This may seem somewhat counter-intuitive since the signal intensity increases with magnetic field strength, which can be traded for an increased resolution, which then would make it easier to see small irregularities at higher field. However, soil particles, air, and water have different magnetic field susceptibilities that cause small-scale field gradients that compete with the imaging gradients. These background gradients increase with field strength and so do the image distortions. Due to the small size of the cysts, in that they themselves also influence the field homogeneity, these larger distortions at higher field make the cysts more difficult to detect at 4.7 T and show up more clearly at 1.5 T.

As mentioned above (Fig. 1C, D), beet rot caused by *R. solani* was also detected by MRI in the advanced stages of plant development (Fig. 4). RCRR developed above the inoculum (flat layer around the beet) and was difficult to detect on the beet before removal from the soil. However, the beginning of surface rot was clearly visible on the MRI image (Fig. 4A). This is shown in a selected cross-section of the beet (Fig. 5) where the infected region penetrates 2 mm into the beet, roughly parallel to the surface. Facing the rotting of the beet, a bright layer of mycelia was visible in the MRI image (Fig. 5). This mucous mycelium–soil mix was visible on the beet at harvest but was lost due to washing the plant. The bright region below the beet shows the inoculation site.

Destructive plant–pathogen evaluation

Significant differences in plant weights were observed among treatments (Table 1). Fresh leaf, beet, and root weights were lowest for the treated plants with the concomitant presence of BCN and RCRR. Root length was also lower for the co-infection treatment.

A statistical interaction between *H. schachtii* and *R. solani* was only detected in root fresh weight ($F=30.7$; $df=1$; $P <0.01$). Fresh leaf, root weight, and root length
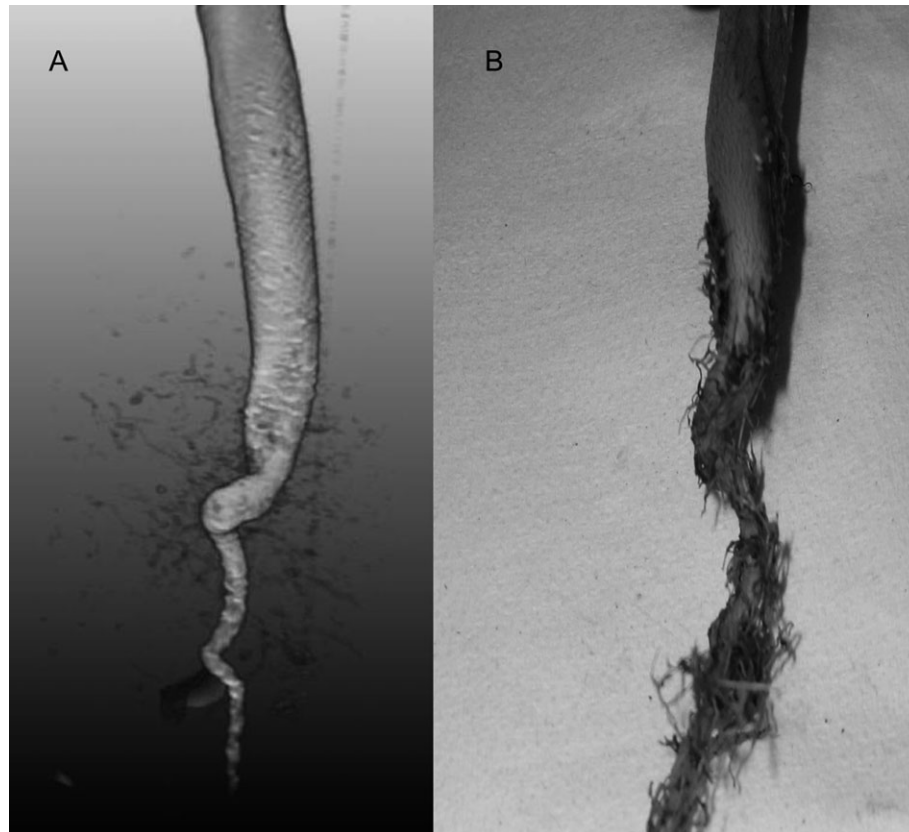
Fig. 2. Three-dimensional nuclear magnetic resonance image recorded from the growing plant in soil (A) and RGB reference image after washing off the soil (B) of a healthy sugar beet root system 56 d after inoculation. Field of view, 76.8×25.6×25.6 mm; resolution, 200×200×400 μm. TE=4 ms, TR=300 ms, measured at 4.7 T.

were impacted synergistically according to the synergy factor (Table 2).

The numbers of BCN eggs and J2s per plant were significantly lower in the disease complex when compared with *H. schachtii* inoculated alone (Table 3). Conversely, the severity of *R. solani* rotting of the beets was more severe in the disease complex treatment than in the treatment with *R. solani* alone (Table 3).

Discussion

This study showed the potential of MRI technology to detect modifications in sugar beet growth due to infections by a pathogen and a nematode. The technique may provide valuable insight into dynamic plant–pathogen interactions in the near future. This is the first report on the use of MRI for non-destructive detection of symptoms caused by BCN on sugar beet.

The production of the 'bearded' root symptom on sugar beet is reported to be caused by *H. schachtii* infection; it has been shown that most of these extra roots lead to loss of resources and drain the plants' energy (Cooke, 1993). The first profusely branched lateral roots were detected in NMR images near the site of J2 inoculation. This finding contrasts with that of Moriarty (1964) who reported that juveniles only penetrate in the elongation zone behind the root tip. It

appears that the nematodes actually penetrate the plant wherever they come into contact. With 3D MRI images it was possible to detect cysts attached to the roots and the beet. This is an important finding that may be applied in breeding for resistance to cyst nematodes and root-knot nematodes, which affect a wide range of economically important crops.

Decay on the beet of *R. solani*-inoculated plants caused cells to leak water which decreased water content of the tissue and, therefore, a decreased MRI signal intensity followed. In this study, inoculum on the soil initiated rotting on the beet at the soil surface, but not at the petioles as reported by Richards (1921) and Herr (1996). Hence, RCRR symptoms were exclusively detected above the source of inoculum when inoculated without *H. schachtii*. Under natural conditions in the field, however, splash water could transfer the fungal inoculum to the petioles and cause symptoms as described (Herr, 1996).

The assumption that fungal penetration is stimulated by nematode root damage (Polychronopoulos *et al.*, 1969; Bergeson, 1972) was confirmed with the MRI image of plants inoculated concomitantly. When nematodes were present on plants, RCRR developed below and above the inoculation site, in contrast to plants inoculated with *R. solani* only where development of RCRR was exclusively above the inoculum. The distinct development of RCRR
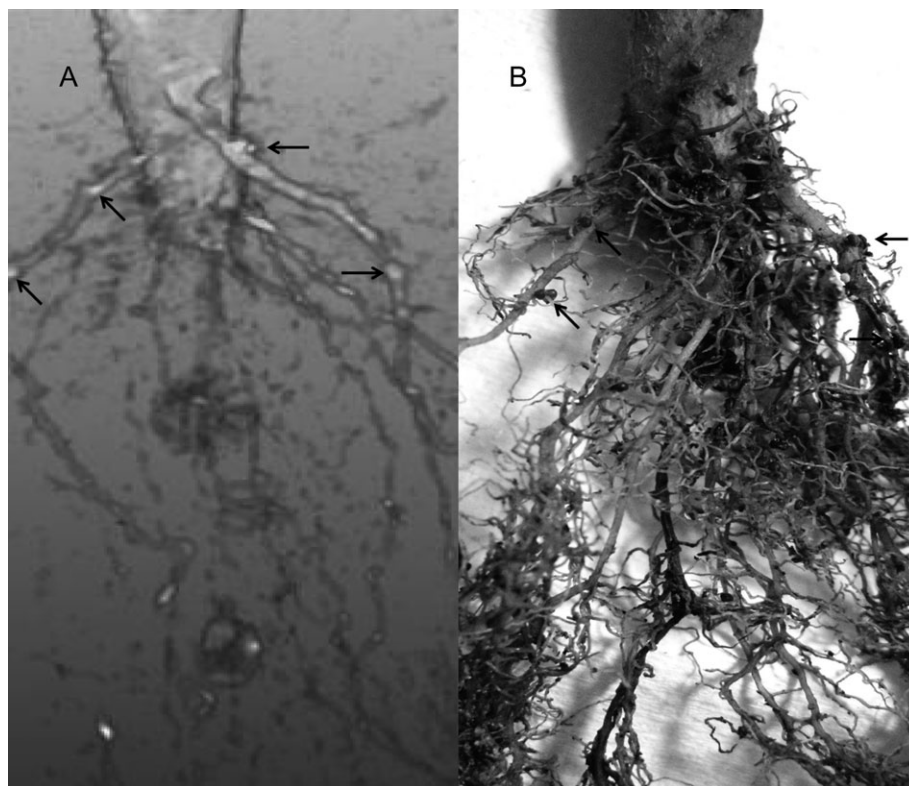
Fig. 3. Three-dimensional nuclear magnetic resonance image recorded from the growing plant in soil (A) and RGB reference image after washing off the soil (B) of a *Heterodera schachtii* inoculated sugar beet root system 56 d after inoculation. Field of view, 76.8×25.6×25.6 mm; resolution, 200×200×400 µm. TE=5 ms, TR=600 ms, measured at 1.5 T.
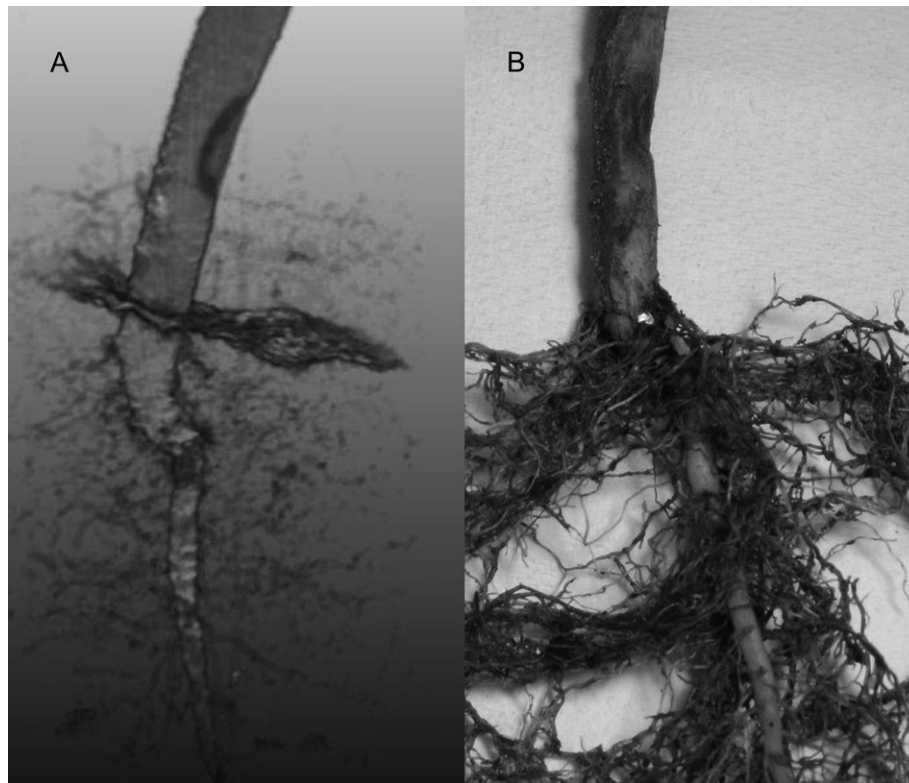

Fig. 4. Three-dimensional nuclear magnetic resonance image recorded from the growing plant in soil (A) and RGB reference image after washing off the soil (B) of a sugar beet root system inoculated with *Rhizoctonia solani* 56 d after inoculation. Field of view, 76.8×25.6×25.6 mm; resolution, 200×200×400 µm. TE=4 ms, TR=300 ms, measured at 4.7 T.

Fig. 5. Three-dimensional nuclear magnetic resonance image cross-section of the same sugar beet root system inoculated with *Rhizoctonia solani* as shown in Fig. 4, 56 d after inoculation. Field of view, 76.8×25.6×25.6 mm; resolution, 200×200×400 µm. TE=4 ms, TR=300 ms, measured at 4.7 T.

Table 1. Influence of *Heterodera schachtii* and *Rhizoctonia solani* alone or in combination on plant fresh weights and root length of sugar beet plants 56 d after inoculation

Treatment	Leaf weight (g)	Root weight (g)	Beet weight (g)	Root length (cm)
Control	25.8±0.9 a	6.5±0.7 b	12.9±1.9 a	2687±81 a
Heterodera schachtii	15.6±0.3 a,b	9.9±0.7 a	5.6±0.3 b	2786±191 a
Rhizoctonia solani	9.8±6.7 b,c	1.7±1.1 c	3.7±2.4 b	35±4 b
H. schachtii+R. solani	0.3±0.1 c	0.2±0.1 c	0.4±0.1 b	18±4 b

Displayed are the means ±SE. Different letters indicate a significant difference after Tukey's test ($P <0.05$; $n=5$).

Table 2. Synergy factor of the effect of the disease complex of *Heterodera schachtii* and *Rhizoctonia solani* on the fresh weight of leaves, roots, and beet, as well as on root length 56 d after inoculation
A synergy factor >1.0 indicates synergistic effects among organisms.

Plant parameter	Synergy factor
Leaf fresh weight	1.1
Root fresh weight	1.3
Beet fresh weight	0.8
Root length	1.1

below the site of fungal inoculation seemed to be correlated to the root region damaged or predisposed by nematode

Table 3. Number of juveniles (J2s) and eggs of *Heterodera schachtii*-inoculated treatments, and *Rhizoctonia solani*-caused beet rot rating of inoculated treatments 56 d after inoculation

Treatment	Number of eggs and J2s	*R. solani* beet rot rating
Heterodera schachtii	10, 249±208 b	–
Rhizoctonia solani	–	2.45±0.31 a
H. schachtii+R. solani	4,438±116 a	4.93±0.21 b

Displayed are the means ±SE. Different letters indicate a significant difference after *t*-test ($P <0.05$; $n=5$).

penetration. Signal intensity was lower and surface rot on the beet was higher when compared with plants exclusively infected by *R. solani*. Lower BCN numbers in the disease complex treatment could be explained by the presence of additional root rot and the decreased numbers of roots serving as host for the obligate parasite.

As reported by Hillnhütter *et al.* (2011) synergistic damage by the disease complex to plants was detected. Significant differences in plant fresh weight were observed among treatments. Nevertheless, during termination and removal of the sugar beet plants from the PVC tubes used in the experiments, many of the tender lateral roots were inadvertently lost. The loss of these roots in normal experimentation leads to inexact data on root growth and the effects of pathogens and or nematodes on real root growth. It underscores the advantage of using a non-destructive technique such as MRI to investigate soil-borne pathogens on plant root systems (Chudek and Hunter, 1997; Köckenberger, 2001; Nagel *et al.*, 2009).

Conclusions

This is the first report of the detection of damage caused by BCN and RCRR on sugar beet and the development of a synergistic disease complex by non-destructive MRI. The results could be important for early detection of damage before visual symptoms are detectable when infection processes occur in the soil. The non-destructive nature of MRI technology will give fundamental insight into the presence of cultivar resistance to soil-borne fungal pathogens and plant-parasitic nematodes at different times after infection, and allow protection of valuable germplasm for differentiation of genotypes for different mechanisms of resistance and susceptibility. Combination of MRI with positron emission tomography (PET) in order to assess not only structure, but also physiological effects (e.g. tolerance of genotypes to infection, i.e. yield formation despite the presence of pathogens), is needed. Further experimentation is needed to increase the resolution of the MRI system in order to identify the giant cells in the roots by

the non-destructive system. Also, research should look more closely at the development of RCRR in the beet prior to the rotting process.

Acknowledgements

References

Abbott WS. 1925. A method of computing the effectiveness of an insecticide. *Journal of Economic Entomology* **18,** 265–267.

Amiri S, Subbotin SA, Moens M. 2002. Identification of the beet cyst nematode *Heterodera schachtii* by PCR. *European Journal of Plant Pathology* **108,** 497–506.

Ayoub S.M. 1980. *Plant nematology—an agricultural training aid*. Sacramento, CA: NemaÁid Publication.

Back MA, Haydock PPJ, Jenkinson P. 2006. Interactions between the potato cyst nematode *Globodera rostochiensis* and diseases caused by *Rhizoctonia solani* AG3 in potatoes under field conditions. *European Journal of Plant Pathology* **114,** 215–223.

Baker KF. 1970. Types of *Rhizoctonia* diseases and their occurrence. In: Parmeter JR, ed. *Rhizoctonia solani: biology and pathology*. Los Angeles, CA: University of California Press, 125–148.

Berdugo CA. 2009. Establishment of a screening test for resistance of sugar beet to *Rhizoctonia solani* AG 2-2IIIB and AG 4. *MSc Thesis,* University of Bonn, Germany, 51.

Bergeson BB. 1972. Concepts of nematode–fungus associations in plant disease complexes: a review. *Experimental Parasitology* **32,** 301–314.

Bleve-Zachero T, Zachero G. 1987. Cytological studies of the susceptible reaction of sugar beet roots to *Heterodera schachtii*. *Physiological and Molecular Plant Pathology* **30,** 13–25.

Bloch D, Hoffmann C. 2005. Seasonal development of genotypic differences in sugar beet (*Beta vulgaris* L.) and their interaction with water supply. *Journal of Agronomy & Crop Science* **191,** 263–272.

Blümler P, Windt CW, van Dusschoten D. 2009. Magnetic resonance of plants. *Nova Acta Leopoldina* **357,** 17–30.

Büttner G, Pfähler B, Märländer B. 2004. Greenhouse and field techniques for testing sugar beet for resistance to *Rhizoctonia* root and crown rot. *Plant Breeding* **123,** 158–166.

Chudek JA, Hunter G. 1997. Magnetic resonance imaging of plants. *Progress in Nuclear Magnetic Resonance Spectroscopy* **31,** 43–62.

Cooke DA. 1987. Beet cyst nematode (*Heterodera schachtii* Schmidt) and its control on sugar beet. *Agricultural Zoology Reviews* **2,** 135–183.

Cooke DA. 1993. Nematode parasites of sugarbeet. In: Evans K, Trudgill DL, Webster JM, eds. *Plant parasitic nematodes in temperate agriculture*. Wallingford, UK: CABI Publishing, 133–170.

Decker H. 1969. *Phytonematologie—Biologie und Bekämpfung pflanzenparasitärer Nematoden.* Berlin, Deutscher Landwirtschaftsverlag, 231–239.

Edzes H, van Dusschoten D, van As, H. 1998. Quantitative T2 imaging of plant tissues by means of multi-echo MRI microscopy. *Magnetic Resonance Imaging* **16,** 185–196.

Eliasson L, Bollmark M. 1988. Ethylene as a possible mediator of light-induced inhibition of root growth. *Physiologia Plantarum* **72,** 605–609.

Gossuin Y, Hocq A, Gillis P, Vuong QL. 2010. Physics of magnetic resonance imaging: from spin to pixel. *Journal of Physics D: Applied Physics* **43,** 1–15.

Haacke EM, Brown RW, Thompson MR, Venkatesan R. 1999. *Magnetic resonance imaging—physical principles and sequence design*. New York: John Wiley & Sons.

Halloin JM, Cooper TG, Potchen EJ. 1992. A study of disease development in *Rhizoctonia solani*-infected sugarbeets using magnetic resonance imaging. *Phytopathology* **82:** 1160.

Herr LJ. 1996. Sugar beet diseases incited by *Rhizoctonia* species. In: Sneh B, Jabaji-Hare S, Neate S, Dijst G, eds. *Rhizoctonia species: taxonomy, molecular biology, ecology, pathology and disease control*. Dordrecht, The Netherlands: Kluwer Academic Publishers, 341–349.

Hillnhütter C, Sikora RA, Oerke E- C. 2011. Influence of different levels of resistance or tolerance in sugar beet cultivars on complex interactions between *Heterodera schachtii* and *Rhizoctonia solani*. *Nematology* **13,** 319–332.

Hooper DJ, Hallmann J, Subbotin S. 2005. Methods for extraction, processing and detection of plant and soil nematodes. In: Luc M, Sikora RA, Bridge J, eds. *Plant parasitic nematodes in subtropical and tropical agriculture*. Wallingford, UK: CABI Publishing, 53–86.

Hummel GM, Schurr U, Baldwin IT, Walter A. 2009. Herbivore-induced jasmonic acid bursts in leaves of *Nicotiana attenuata* mediate short-term reductions in root growth. *Plant, Cell and Environment* **32,** 134–143.

Jahnke S, Menzel MI, van Dusschoten D, et al. 2009. Combined MRI–PET dissects dynamic changes in plant structures and functions. *The Plant Journal* **59,** 634–644.

Köckenberger W. 2001. Functional imaging of plants by magnetic resonance experiments. *Trends in Plant Science* **6,** 286–292.

Kuchenbrod E, Haase A, Benkert R, Schneider H, Zimmermann U. 1995. Quantitative NMR microscopy of intact plants. *Magnetic Resonance Imaging* **13,** 447–455.

MacFall JS, Spaine P, Doudrick R, Johnson GA. 1994. Alterations in growth and water-transport processes in fusiform rust galls of pine, determined by magnetic resonance microscopy. *Phytopathology* **84,** 288–293.

Müller J. 1980. Ein verbessertes Extraktionsverfahren für *Heterodera schachtii*. *Nachrichtenblatt Deutscher Pflanzenschutzdienst* **3,** 21–24.

Moriarty F. 1964. The monoxenic culture of beet eelworm (*Heterodera schachtii* Schm.) on excised roots of sugar beet (*Beta vulgaris* L.). *Parasitology* **54,** 289–293.

Nagel KA, Kastenholz B, Jahnke S, *et al*. 2009. Temperature response of roots: impact on growth, root system architecture and implications for phenotyping. *Functional Plant Biology* **36,** 947–959.

Oostenbrink M. 1960. Estimating nematode populations by some elected methods. In: Sasser JN, Jenkins WR, eds. *Nematology*. Chapel Hill, NC: University of North Carolina Press, 85–102.

Polychronopoulos AG, Houston BR, Lownsberry BF. 1969. Penetration and development of *Rhizoctonia solani* in sugar beet seedlings infected with *Heterodera schachtii*. *Phytopathology* **59,** 482–485.

Richards BL. 1921. A dry rot cancer of sugar beets. *Journal of Agricultural Research* **22,** 47–67.

Scheenen TWJ, van Dusschoten D, de Jager PA, van As H. 2000. Quantification of water transport in plants with NMR imaging. *Journal of Experimental Botany* **51,** 1751–1759.

Shurtleff MC, Averre CW. 1997. *Glossary of plant-pathological terms*. St Paul, MN: American Phytopathological Society Press.

Sikora RA, Carter WW. 1987. Nematode interactions with fungal and bacterial plant pathogens—fact or fantasy. In: Veech JA, Dickson DW, eds. *Vistas on nematology*. Hyattsville, MD: Society of Nematologists, 307–312.

van As H, Windt, CW. 2008. Magnetic resonance imaging of plants: water balance and water transport in relation to photosynthetic activity. In: Aartsma J, Matysik J, eds. *Biophysical techniques in photosynthesis II*, Vol. 26. Berlin: Springer, 55–73.

Weishaupt D. 2001. *Wie funktioniert MRI?* Berlin: Springer.

Wyss U. 1992. Observations on the feeding behaviour of *Heterodera schachtii* throughout development, including events during moulting. *Fundamental and Applied Nematology* **15,** 75–89.

Wyss U. 1997. Root parasitic nematodes—an overview. In: Fenoll C, Grundler FMW, Ohl SA, eds. *Cellular and molecular aspects of plant–nematode interactions*. Wageningen, The Netherlands: Kluwer Academic Publishers, 5–22.

Zens I, Steiner U, Dehne HW. 2002. Auftreten, Charakterisierung und Kontrolle des Erregers der Rübenfäule, *Rhizoctonia solani*, in Nordrhein-Westfalen. *Landwirtschaftliche Fakultät der Universität Bonn, Schriftenreihe des Lehr- und Forschungsschwerpunktes USL* **91,** 1–99.